Rest functional brain maturation during the first year of life

Pierre Augé[a†] and Hervé Lemaître[a,b†*], Ana Saitovitch[a], Jean-Marc Tacchella[a], Ludovic Fillon[a], Raphael Calmon[a], Raphaël Lévy[a], David Grévent[a], Francis Brunelle[a], Nathalie Boddaert[a], Monica Zilbovicius[a]

Author affiliation

"a" INSERM U1000, Department of Pediatric Radiology, Hôpital Necker Enfants Malades, AP-HP, Imagine Institute (UMR 1163), Paris Descartes University, Sorbonne Paris Cité University.

"b" Faculté de Médecine, Paris-Sud University, University of Paris-Saclay.

† Both authors contributed equally for this work

*Correspondence and material request should be addressed to Hervé Lemaître (herve.lemaitre@u-psud.fr)

Keywords

Infants brain maturation

Rest cerebral blood flow

Neurodevelopment

ASL-MRI

Summary

The first year of life is a key period of brain development, characterized by dramatic structural and functional modifications. Here, we measured rest cerebral blood flow (CBF) modifications throughout babies' first year of life using arterial spin labeling magnetic resonance imaging sequence in 52 infants, from 3 to 12 months of age. Overall, global rest CBF significantly increased during this age span. In addition, we found marked regional differences in local functional brain maturation. While primary sensorimotor cortices and insula showed early maturation, temporal and prefrontal region presented great rest CBF increase across the first year of life. Moreover, we highlighted a late and remarkably synchronous maturation of the prefrontal and posterior superior temporal cortices. These different patterns of regional cortical rest CBF modifications reflect a timetable of local functional brain maturation and are consistent with baby's cognitive development within the first year of life.

Introduction

The human brain is still immature at birth and undergoes dynamic structural and functional processes throughout life. During the first year, the maturation of neural networks is a complex process that is particularly important to the baby's acquisition of cognitive and motor skills (1). At the cortical level, development comprises both gross morphometric changes and microstructural progression (2). The first year of life is therefore a critical phase of postnatal brain development.

Historically, much of what we know about the intricate processes of early brain development comes from post-mortem studies in human fetuses, neonates, and non-human primates (3-5). With the increasing availability of high-quality neuroimaging techniques, studying early human brain development in vivo in unprecedented detail is now feasible (6-9). These advances have led to exciting new insights into both healthy and atypical macroscale brain network development and have paved the way to bridge the gap between the brain's neurobiological architecture and its behavioral repertoire.

At the structural level, in neonates and infants, studies of cortical morphological development have focused on the modification of gray matter volume (10, 11), gyrification (12), deep sulcal landmark maturation (13), thickness and surface area maturation (14), as well as folding and fiber density (15). Structural brain imaging studies showed an increase in the gray matter volume during the first years of life (11), consistent with post-mortem studies, indicating rapid development of synapses and spines during this period (16-18). Indeed, throughout late gestation, rapid synaptogenesis results in an over-abundance of synapses (up to 150% of adult values) that are subsequently pruned throughout childhood and adolescence (19). During the first year of life, synaptogenesis is one of the most important maturational processes, and its timetable differs across cortical regions. Gilmore et al. described a posterior to anterior gradient of gray matter growth throughout the first year of life (20), consistent with regional differences that have been described in post-mortem studies, showing an increase in synaptic density, and therefore synaptogenesis, earlier in the sensory cortex and later in the prefrontal cortex (16). In general, studies have suggested a complex pattern of development that varies based on anatomical location and cortical metrics. In addition, across early development, cortical maturation exhibits

62 regionally specific asymmetry between the left and right hemispheres (12, 15). These
63 changes continue throughout childhood and adolescence, with cortical thickness following
64 different trajectories of thinning depending on the region, cortex type and gender (21, 22).

65 At the functional level, early brain development has been investigated using mainly three
66 different approaches. Pioneer studies measuring metabolism and rest cerebral blood flow
67 (CBF) were followed by activation studies using functional MRI and more recently resting
68 state MRI studies investigating functional connectivity.

69 Rest cerebral metabolism and blood flow are an index of synaptic density, which allows the
70 in vivo study of functional brain maturation using positron emission tomography (PET) and
71 single-photon emission computed tomography (SPECT) (23). These studies revealed that
72 infants' brains showed higher rest metabolism in subcortical structures and in the
73 sensorimotor cortex than in other regions (24). In the newborn, the highest degree of
74 glucose metabolism is in the primary sensory and motor cortex, cingulate cortex, thalamus,
75 brain stem, cerebellar vermis and hippocampal region. During the first months of life, rest
76 metabolism and CBF increase firstly within the primary sensory cortices, followed by the
77 associative sensory cortices and finally within the prefrontal cortex at the end of the first
78 year (24-26). At 2 to 3 months of age, glucose utilization increases in the parietal, the
79 temporal and the primary visual cortices, basal ganglia, and cerebellar hemispheres.
80 Between 6 and 12 months of age, glucose utilization increases in the frontal cortex. These
81 metabolic changes correspond to the emergence of motor and cognitive abilities during the
82 first year of life. However, these studies were limited by very low spatial resolution of the
83 brain imaging devices. In addition, these techniques required administration of ionizing
84 radiation and, therefore, have limited application in the pediatric population.

85 Following these pioneer studies, task-based fMRI contributed to present-day knowledge
86 about brain maturation shortly after birth (27-29). These studies have provided important
87 background on the brain's responses to sensory input during the early developmental phases
88 of brain-behavior interactions. Adult-like activation patterns were observed in response to a
89 variety of sensory stimuli, including tactile and proprioceptive stimulation (passive hand
90 movement) (28, 30) as well as auditory (31) and olfactory (the odor of infant formula) (32).
91 Functional MRI studies in 2- to 3-month-old infants demonstrated left-lateralized activation

of perisylvian regions, including the superior temporal gyrus, angular gyrus and Broca's area, in response to native language speech. The response followed a hierarchical pattern, with auditory regions being activated first, followed by superior temporal regions, the temporal poles and Broca's area in the inferior frontal cortex; a pattern that is highly consistent with language organization in the mature brain (29).

More recently, advances in brain imaging methodology have led to expanded application of resting state functional MRI (rs-fMRI) to the study of infants during the first years of life, providing insight into the maturation of multiple resting state networks (RSNs). Results show that the rate at which correlations within and between RSNs develop differs by network and closely reflect known rates of cortical development based on histological evidence (33). The sensorimotor (SM) and attention (AN) networks seem to be the earliest developing networks with their within-network synchronization largely established before birth. This replicates several reports showing the bilateral symmetric, adult-like topology of both networks at birth (34, 35) or even prenatally (36), indicating significant prenatal development of these 2 networks. In the brains of term babies, rs-fMRI studies employing seed-based connectivity or independent component analyses have identified specific functional networks, including primary visual, auditory, sensorimotor networks and default mode and executive-control networks involved in heteromodal functions (7, 36, 37). Network analyses based on graph theory further revealed that the functional connectomes of infant brains already exhibited the small-world structure. Distinct from the adults, however, the hubs were largely confined to primary sensorimotor regions (38, 39). Taken together, these findings provide important insights into the early brain functional maturation process.

The emergence of arterial spin labeling (ASL), a technique that provides both non-invasive and regional cerebral blood flow quantification, offers new opportunities to investigate local rest brain function in neonates and children. ASL perfusion MRI uses magnetically labeled arterial blood water as a nominally diffusible flow tracer. By labeling the blood water proximal to the target imaging region, the perfusion signal is subsequently calculated by comparison with a separate image acquired using a control pulse without labeling the blood flow to remove the static background signal and control for magnetization transfer effects (40). Therefore, ASL MRI non-invasively assesses brain perfusion and allows for a quantitative measurement of rest CBF without the administration of contrast material or

exposure to ionizing radiation (41). This imaging method has been used to study rest CBF in neonates (42, 43), toddlers (44, 45) and older children (46), as well as, more recently, brain injuries in preterm babies (47).

Despite its importance for understanding normal brain development, we lack in knowledge of the development of local rest brain function characteristics during the first year of life. In this study, we aimed to describe the modifications of local rest CBF at the voxel-by-voxel level throughout the first year of life using ASL perfusion MRI.

Results

The relative values of global rest CBF increased with age from 3 to 12 months in the right (b = 0.0010 unit/year, $t_{(55.71)}$ = 6.64, p = 1.36E-08) and in the left hemisphere (b = 0.00078 unit/year, $t_{(55.71)}$ = 5.34, p = 1.74E-06) with a greater age-related increase in the right as compared to the left (p = 0,0074, see Figure 1 and Table 1).

Qualitative analysis of the whole-brain voxel-wise maps showed a regionally heterogeneous age-related increase of the relative rest CBF values (see Figure 2 and SI Appendix, Movies S1 to S4). The highest rest CBF at 3 months were observed within the sensorimotor and the primary visual cortices. The age-related increase in rest CBF progressed spatially from these regions. From the calcarine fissure, the rest CBF increased toward the visual associative regions up to the supramarginal and the precuneus regions. From the primary motor and sensory cortices, the rest CBF increased toward both the anterior and the posterior part of the brain. Anteriorly, through the anterior cingulate and the prefrontal cortices; posteriorly, through the insula and the superior temporal cortices. In contrast, the rest CBF was stable within the thalamus, the amygdala and the hippocampus. Between 9 and 12 months, the rest CBF increase was predominantly seen in the temporal and the prefrontal cortices. The regional right over left rest CBF asymmetry remained present throughout the whole studied period.

Quantitative analysis within the predefined regions of interest showed different trajectories of local rest functional maturation (see Table 1 and Figure 1). First, in a subset of subcortical regions including the hippocampus (right: b = 0.00019 unit/year, $t_{(75.14)}$ = 1.52, p = 1; left: b = -0.00022 unit/year, $t_{(75.14)}$ = -1.71, p = 0,82), the amygdala (right: b = 0.000026 unit/year,

152 $t_{(92.77)}$ = 0.18, p = 1; left: b = -0.000076 unit/year, $t_{(92.77)}$ = -0.54, p = 1) and the thalamus
153 (right: b = -0.00031 unit/year, $t_{(66.29)}$ = -2.62, p = 0,097; left: b = -0.00043 unit/year, $t_{(66.29)}$ = -
154 3.66, p = 0.0045), the age-related rest CBF maturation through the first year of life remained
155 stable indicating already matured regions at 3 months old. Second, the subset of cortical
156 regions including the primary visual (right: b = 0.00094 unit/year, $t_{(59.09)}$ = 4.36, p = 0.00047;
157 left: b = 0.00085 unit/year, $t_{(59.09)}$ = 3.94, p = 0.0020) and primary auditory cortices (right: b =
158 0.00032 unit/year, $t_{(75.03)}$ = 1.64, p = 0.94; left: b = 0.00015 unit/year, $t_{(75.03)}$ = 0.78, p = 1), the
159 insula (right: b = 0.00057 unit/year, $t_{(82.2)}$ = 4.29, p = 0.00044, left: b = 0.00028 unit/year,
160 $t_{(82.2)}$ = 2.06, p = 0.38) and the sensorimotor cortex (right: b = 0.00061 unit/year, $t_{(59.33)}$ =
161 2.89, p = 0.048; left: b = 0.00025 unit/year, $t_{(59.33)}$ = 1.19, p = 1) presented a small age-related
162 rest CBF increase indicating early maturational process. Third, a subset of cortical regions
163 including the prefrontal (right: b = 0.0014 unit/year, $t_{(58.9)}$ = 6.9, p = 3.64E-08; left: b = 0.0012
164 unit/year, $t_{(58.9)}$ = 6.26, p = 4.31E-07) and the superior temporal cortices (right: b = 0.00095
165 unit/year, $t_{(61.7)}$ = 5.4, p = 1.00E-05; left: b = 0.00060 unit/year, $t_{(61.7)}$ = 3.41, p = 0.010)
166 presented a high age-related rest CBF increase indicating late maturational process. Finally,
167 faster right over left age-related rest CBF increase was more pronounced within the superior
168 temporal (p = 0.032) and sensorimotor cortices (p = 0.05).

169 The age-related rest CBF changes computed for the exhaustive list of 45 regions of interest
170 are available in SI Appendix, Table S3.

171

172 **Discussion**

173 Our study shows for the first time the dynamics of local rest functional brain maturation
174 throughout the first year of life using a high-resolution non-invasive imaging method. Global
175 rest CBF increased significantly from 3 to 12 months of age and this increase was more
176 pronounced in the right than in the left hemisphere. Qualitative and quantitative analyses
177 revealed marked regional differences in local functional brain maturation. Subcortical
178 structures such as basal ganglia, thalamus, amygdala and hippocampus cortices are
179 functionally mature at 3 months. At the cortical level, we observed two different
180 maturational trajectories. Firstly, almost functionally mature regions at 3-month-old, with a
181 slow age-related rest CBF increase between 3 to 12 months, included the primary
182 auditory/visual cortices, the sensorimotor cortex and the insula. Secondly, late functionally

183 mature regions, with a high age-related increase rest CBF increase between 3 to 12 months,
184 included the superior temporal and prefrontal cortices.

185 The increase in global rest CBF from 3 to 12 months of age that we describe here is
186 consistent with pioneers PET and SPECT studies showing increase in rest metabolism and
187 CBF during the same period (25, 26). Furthermore, we highlighted a hemispheric functional
188 maturational asymmetry, with greater right than left global rest CBF increase during the first
189 year. This agrees with previous studies that showed greater right than left rest CBF for these
190 regions at birth (34) and from 1 year to 3 years old (48), supporting the hypothesis that the
191 right hemisphere functionally matures earlier than the left. This asymmetry was also
192 observed regionally for the superior temporal and sensorimotor cortices , consistently with
193 data from rs-fMRI studies, also indicating asymmetry in the maturation of sensorimotor
194 network (49).

195 Globally, our findings are in accordance with results from prior research based on histology,
196 structural and rest functional brain imaging that has revealed distinct maturation trajectories
197 of cortical regions and brain networks over the first year of life (10, 24, 33, 50). Firstly, at the
198 histological level, post-mortem data showed that the time course of synaptogenesis differs
199 across cortical regions. Indeed, a burst of synapse formation occurs between 3 and 4 months
200 within primary visual, auditory cortices somatosensory cortices, which appeared already
201 mature at 3 months of life (16, 51-53). Synaptogenesis in the frontal cortex begins about the
202 same time as in visual cortex, but it does not reach its peak period until age 8 months,
203 continuing thereafter through the second year of life (16, 54). These congruent findings
204 strengthen our results as synaptic density is coupled to rest CBF as measured in our study.
205 Secondly, concerning myelination, microstructural MRI maturational studies described a
206 global maturation pattern characterized by early maturation of the sensorimotor cortex,
207 followed by the other sensory cortices and then the associative cortices, including the
208 prefrontal cortex (55, 56). Finally, recent data obtained with resting-state functional MRI
209 studies allowed to describe maturational changes of functional networks during the first
210 year of life (33, 36, 57, 58). Especially, Gao et al. have described a maturation sequence
211 starting with primary sensorimotor/auditory and visual then attention/default-mode, and
212 finally executive control, prefrontal, networks (57). These different sequences of functional
213 network maturation fit with and complement our results. Therefore, data coming from our

214 study and previous rs-fMRI studies contribute to map a timetable of functional brain
215 maturation during the first year of life.

216 Importantly, the spatial resolution of the ASL images allowed a highly accurate mapping of
217 the age-related rest CBF changes. Consequently, we were able to describe insular local
218 functional maturational evolution, which reaches its one-year pattern rather early, during
219 the first months of life. A well-established literature and recently anatomical and resting-
220 state functional MRI studies describe early human cortical development in areas close to the
221 insula and radiating outward (59). This early insular maturation fits with its role in the
222 integration of interoceptive stimuli, such as coolness, warmth and distension of the bladder,
223 stomach or rectum (60), but also in the integration of external stimuli, notably pain (61). In
224 addition, it is highly pertinent, since the insula is a key structure for the baby's development
225 and essential to baby's survival.

226 The spatial resolution improvement also allowed us to describe for the first time a
227 remarkably synchronous increase in rest CBF between the prefrontal and superior temporal
228 cortices, both main components of the called "social brain" (62). The late maturation of the
229 prefrontal cortex had been previously described by structural and functional brain imaging
230 studies (10, 24). Noticeably, we describe here a late maturation within the posterior
231 temporal regions during the first year of life, particularly within the posterior superior
232 temporal sulcus, a region known to be highly implicated in social cognition (63).
233 Interestingly, the late and synchronous maturation of these two cortical structures
234 corresponds to the remarkable development of the baby's social skills through the first year
235 of life.

236 To the best of our knowledge, only 2 studies using ASL imaging have focused on brain
237 development during the first year of life, but a comparison with our results is limited due to
238 important differences in their methodological approaches. Duncan et al. studied a sample of
239 61 infants within a very narrow age-range from 3 to 5 months (45). Their main results
240 describing a significantly greater rest CBF in the sensorimotor and occipital regions
241 compared with the dorsolateral prefrontal in this age-range are in accordance with our
242 results. In the second study, combining region of interest (ROI) and whole-brain analyses on
243 rest CBF, Wang et al. investigated a group of 8 7-month-old infants to a group of 8 13-

month-old infants (44). Although they showed rest CBF increase in the 13-month-old group compared to the 7-month-old group mainly located in the frontal lobe, they did not examine directly the age-related rest CBF slopes.

This study has some limitations. First, we used a linear model for data analysis. Although cubic and quadratic fitting models did not improve our statistical models, it is improbable that a linear model exactly fits functional cortical maturation. This issue can be addressed in future studies by adding more and older subjects to further investigate the postnatal brain rest functional maturation trajectory. Second, due to their age, all infants received light premedication before the MRI to prevent motion artifacts, and all the scans were acquired during sleep. No significant influence neither on the regional distribution of CBF (7, 37, 64) nor in the default-mode network connectivity (65) has been reported to this premedication. Finally, our study was performed in a clinical pediatric population. To ensure that it could be comparable with a non-clinical population, we discarded all clinical indications for MRI that could affect brain anatomy, function and further neurodevelopmental disorders. In addition, all scans were strictly normal, and follow-up confirmed a normal psychomotor development.

Defining typical trajectories of brain maturation provides references for a better understanding of neurodevelopmental disorders and preterm effects on further brain maturation. Because CBF reflects regional changes in synaptic density, ASL offers a noninvasive approach to studying local brain function. In conclusion, to our knowledge, our study is the first to describe and characterize dynamics local functional brain maturation during the first year of life and provide insight into an important and vulnerable neurodevelopmental period.

Author contributions

P.A. contributed to conception, analysis, interpretation and draft

H.L. contributed to conception, analysis, interpretation and draft

A.S. contributed to conception, interpretation and draft

J-M.T. contributed to analysis and draft

L.F. contributed to interpretation and draft

R.C. contributed to acquisition

R.L. contributed to acquisition

D.G contributed to acquisition

F.B. contributed to acquisition

N.B. contributed to conception and acquisition

M.B. contributed to conception, interpretation and draft

Declaration of Interests

The authors declare no competing interests.

Figure Legends

Figure 1: Age-related changes of the rest CBF values in predefined regions of interest between 3 and 12 months of age. The whole brain in red, subset of stable subcortical regions (hippocampus, amygdala and thalamus) in purple, subset of early maturing cortical regions (primary visual and auditory cortices, insula and sensorimotor cortex) in green, subset of late maturing cortical regions (prefrontal and superior temporal cortices) in blue. Each dot represents a subject, and each line represents the estimated regression based on a linear model for the left (empty dots and dashed line) and right (filled dots and solid line) hemispheres. The rest CBF values are normalized by the rest CBF measured within the basal ganglia and presented in arbitrary unit.

Figure 2: rest CBF values at 3, 6, 9 and 12 months of age displayed on the medial and lateral view of the left and right hemispheres. The rest CBF values are normalized by the rest CBF measured within the basal ganglia and presented in arbitrary unit. Surface rendering was done using mri_vol2surf from freesurfer (https://surfer.nmr.mgh.harvard.edu/).

STAR Methods

Subject. Eighty-five babies from the Necker-Enfants-Malades hospital were initially included in this study. The inclusion criteria were normal clinical multimodal MRI, absence of

prematurity, neurological or cranial pathology, parent's consanguinity or abnormal psychomotor development. Were included infants presenting syndromes that are not originally neurological, mainly dermatological or ophthalmological, but request an MRI to discard infrequent associated brain abnormalities, that may be present in a small percentage of cases (see SI Appendix, Table S1). Normal psychomotor development was assured in follow-up consultations. Our final sample included 52 babies (29 girls) from 3 to 12 months of age in our study, including 10 babies at 3 and 4 months (90 to 120 days), 14 at 5 and 6 months (120 to 180 days), 14 at 7 and 8 months (180 to 240 days), 7 at 9 and 10 months (240 to 300 days), 7 at 11 and 12 months (300 to 375 days). The Ethical Committee of French Public Hospitals approved this study and the written informed consent was obtained for all participants.

MRI acquisition. All MRI exams included T1-weighted and ASL sequences and were acquired on a General Electric Signa 1.5T MRI scanner in the Necker-Enfants-malades hospital (See SI Appendix, Table S2 and SI Methods for details). Due to the age of the babies, all of them received premedication before their MRI (pentobarbital, 7.5 mg/kg) to prevent motion artifacts. It has been shown that barbiturates do not have any influence on the regional distribution of CBF or on default mode resting state network (7, 37, 66, 67).

Data processing and treatment. MRI images were pre-processed using Statistical Parametric Mapping (SPM8 software, Welcome Department of Cognitive Neurology London www.fil.ion.ucl.ac.uk/spm/software/spm8) implemented in Matlab (Mathworks Inc., Sherborn, MA, USA) and analyzed using a voxel-based approach (See SI Appendix, SI Methods for details). Native 3D-T1-weighted images were segmented into gray matter, white matter and cerebrospinal fluid using the Infant Brain Probability Templates (https://irc.cchmc.org/software/infant.php). The ASL images were first co-registered to the corresponding native gray matter images. Then, co-registered ASL images were spatially normalized using the deformation matrices from the segmentation process. The resulting ASL images were smoothed using an isotropic Gaussian filter of 10 mm. ASL acquisition provides a high-quality image of quantitative CBF. Motion in ASL acquisition is mainly characterized by signal outside of the brain, often recognizable as signal from layers of skin or fat, that can be detected by on-the-fly expert visual analysis. Therefore, we performed a two steps quality control. The first one by an expert radiologist right after acquisition (NB)

and the second one by an imaging processing expert engineer (HL) before pre-processing to discard images with artifacts such as motion, aliasing, ghosting, spikes, low signal to noise ratio.

Image analysis. We normalized rest CBF within the ASL images by the mean CBF measured within the basal ganglia to avoid major variations in rest CBF due to cardiac blood flow (68, 69) and blood pressure labilities (70). The basal ganglia was specifically chosen in our study as it is one of the earliest structures to matures (24) and regression analyses did not show any age-related variations in the rest CBF of this region within our age range (beta= 5.2×10^{-4} unit/year, $t_{(50)} = 0.045$, $p = 0.96$). The regional rest CBF was expressed as percentage of basal ganglia rest CBF and presented in arbitrary unit.

We then performed whole-brain voxel-wise analyses of the 52 images within the general linear model framework using SPM8 with age as an independent variable. The analyses were constrained to gray matter tissue only by thresholding the analysis mask to 40% of the mean gray matter image of our sample.

We also extracted mean rest CBF from 92 regions of interest (hemispheres and regions) using the AAL parcellation toolbox (71). In addition, a further analysis was performed by selecting and merging regions of interested based on their relevance in term of development. We selected the hippocampus, the amygdala, the thalamus, the primary visual and auditory cortices, the insula, the superior temporal cortex. We formed the sensorimotor cortex by merging the precentral and postcentral regions, and the prefrontal cortex by merging the inferior, middle and superior frontal regions and the gyrus rectus. All analyses were performed using R (http://cran.r-project.org). Age-related regressions were assessed using linear mixed models to account for the intra-subject left and right hemisphere measurements. Age, hemisphere and age-by-hemisphere interaction were entered as fixed effects and subject as nested random effect.

Data and Code Availability Statement. The data that support the findings of this study are available on request from the corresponding author [HL]. The data are not publicly available due to them containing information that could compromise research participant consent.

References

1. Kagan J & Herschkowitz N (2005) *A Young Mind in a Growing Brain* (Lawrence Erlbaum Associates, Mahwah, NJ, US).
2. Dubois J, *et al.* (2014) The early development of brain white matter: a review of imaging studies in fetuses, newborns and infants. *Neuroscience* 276:48-71.
3. Goldman-Rakic PS (1987) Development of cortical circuitry and cognitive function. *Child Dev* 58(3):601-622.
4. Innocenti GM & Price DJ (2005) Exuberance in the development of cortical networks. *Nat Rev Neurosci* 6(12):955-965.
5. Kostovic I, Judas M, Rados M, & Hrabac P (2002) Laminar organization of the human fetal cerebrum revealed by histochemical markers and magnetic resonance imaging. *Cereb Cortex* 12(5):536-544.
6. Ball G, *et al.* (2014) Rich-club organization of the newborn human brain. *Proc Natl Acad Sci U S A* 111(20):7456-7461.
7. Fransson P, *et al.* (2007) Resting-state networks in the infant brain. *Proc Natl Acad Sci U S A* 104(39):15531-15536.
8. Partridge SC, *et al.* (2004) Diffusion tensor imaging: serial quantitation of white matter tract maturity in premature newborns. *Neuroimage* 22(3):1302-1314.
9. van den Heuvel MP, *et al.* (2015) The Neonatal Connectome During Preterm Brain Development. *Cereb Cortex* 25(9):3000-3013.
10. Gilmore JH, *et al.* (2012) Longitudinal development of cortical and subcortical gray matter from birth to 2 years. *Cereb Cortex* 22(11):2478-2485.
11. Knickmeyer RC, *et al.* (2008) A structural MRI study of human brain development from birth to 2 years. *J Neurosci* 28(47):12176-12182.
12. Li G, *et al.* (2014) Mapping longitudinal development of local cortical gyrification in infants from birth to 2 years of age. *J Neurosci* 34(12):4228-4238.
13. Meng Y, Li G, Lin W, Gilmore JH, & Shen D (2014) Spatial distribution and longitudinal development of deep cortical sulcal landmarks in infants. *Neuroimage* 100:206-218.
14. Lyall AE, *et al.* (2015) Dynamic Development of Regional Cortical Thickness and Surface Area in Early Childhood. *Cereb Cortex* 25(8):2204-2212.
15. Nie J, *et al.* (2014) Longitudinal development of cortical thickness, folding, and fiber density networks in the first 2 years of life. *Hum Brain Mapp* 35(8):3726-3737.
16. Huttenlocher PR & Dabholkar AS (1997) Regional differences in synaptogenesis in human cerebral cortex. *J Comp Neurol* 387(2):167-178.
17. Petanjek Z, *et al.* (2011) Extraordinary neoteny of synaptic spines in the human prefrontal cortex. *Proc Natl Acad Sci U S A* 108(32):13281-13286.
18. Webster MJ, Elashoff M, & Weickert CS (2011) Molecular evidence that cortical synaptic growth predominates during the first decade of life in humans. *Int J Dev Neurosci* 29(3):225-236.
19. Huttenlocher PR (1979) Synaptic density in human frontal cortex - developmental changes and effects of aging. *Brain Res* 163(2):195-205.
20. Gilmore JH, *et al.* (2007) Regional gray matter growth, sexual dimorphism, and cerebral asymmetry in the neonatal brain. *J Neurosci* 27(6):1255-1260.
21. Shaw P, *et al.* (2008) Neurodevelopmental trajectories of the human cerebral cortex. *J Neurosci* 28(14):3586-3594.
22. Sowell ER, *et al.* (2004) Longitudinal mapping of cortical thickness and brain growth in normal children. *J Neurosci* 24(38):8223-8231.
23. Leenders KL, *et al.* (1990) Cerebral blood flow, blood volume and oxygen utilization. Normal values and effect of age. *Brain* 113 (Pt 1):27-47.

24. Chugani HT & Phelps ME (1986) Maturational changes in cerebral function in infants determined by 18FDG positron emission tomography. *Science* 231(4740):840-843.
25. Chugani HT, Phelps ME, & Mazziotta JC (1987) Positron emission tomography study of human brain functional development. *Ann Neurol* 22(4):487-497.
26. Chiron C*, et al.* (1992) Changes in regional cerebral blood flow during brain maturation in children and adolescents. *Journal of nuclear medicine : official publication, Society of Nuclear Medicine* 33(5):696-703.
27. Allievi AG*, et al.* (2016) Maturation of Sensori-Motor Functional Responses in the Preterm Brain. *Cereb Cortex* 26(1):402-413.
28. Arichi T*, et al.* (2010) Somatosensory cortical activation identified by functional MRI in preterm and term infants. *Neuroimage* 49(3):2063-2071.
29. Dehaene-Lambertz G*, et al.* (2006) Functional organization of perisylvian activation during presentation of sentences in preverbal infants. *Proc Natl Acad Sci U S A* 103(38):14240-14245.
30. Erberich SG*, et al.* (2006) Somatosensory lateralization in the newborn brain. *Neuroimage* 29(1):155-161.
31. Anderson AW*, et al.* (2001) Neonatal auditory activation detected by functional magnetic resonance imaging. *Magn Reson Imaging* 19(1):1-5.
32. Arichi T*, et al.* (2013) Computer-controlled stimulation for functional magnetic resonance imaging studies of the neonatal olfactory system. *Acta Paediatr* 102(9):868-875.
33. Smyser CD & Neil JJ (2015) Use of resting-state functional MRI to study brain development and injury in neonates. *Semin Perinatol* 39(2):130-140.
34. Lin PY*, et al.* (2013) Regional and hemispheric asymmetries of cerebral hemodynamic and oxygen metabolism in newborns. *Cereb Cortex* 23(2):339-348.
35. Gao W*, et al.* (2013) The synchronization within and interaction between the default and dorsal attention networks in early infancy. *Cereb Cortex* 23(3):594-603.
36. Smyser CD*, et al.* (2010) Longitudinal analysis of neural network development in preterm infants. *Cereb Cortex* 20(12):2852-2862.
37. Doria V*, et al.* (2010) Emergence of resting state networks in the preterm human brain. *Proc Natl Acad Sci U S A* 107(46):20015-20020.
38. Fransson P, Aden U, Blennow M, & Lagercrantz H (2011) The functional architecture of the infant brain as revealed by resting-state fMRI. *Cereb Cortex* 21(1):145-154.
39. Gao W*, et al.* (2011) Temporal and spatial evolution of brain network topology during the first two years of life. *PLoS One* 6(9):e25278.
40. Williams DS, Detre JA, Leigh JS, & Koretsky AP (1992) Magnetic resonance imaging of perfusion using spin inversion of arterial water. *Proceedings of the National Academy of Sciences of the United States of America* 89(1):212-216.
41. Detre JA & Alsop DC (1999) Perfusion magnetic resonance imaging with continuous arterial spin labeling: methods and clinical applications in the central nervous system. *Eur J Radiol* 30(2):115-124.
42. Ouyang M*, et al.* (2017) Heterogeneous increases of regional cerebral blood flow during preterm brain development: Preliminary assessment with pseudo-continuous arterial spin labeled perfusion MRI. *Neuroimage* 147:233-242.
43. De Vis JB (2012) Arterial Spin Labeling Magnetic Resonance Imaging to Assess Neonatal Brain Perfusion. *Archives of Disease in Childhood* 97.
44. Wang Z*, et al.* (2008) Assessment of functional development in normal infant brain using arterial spin labeled perfusion MRI. *Neuroimage* 39(3):973-978.
45. Duncan AF*, et al.* (2014) Regional cerebral blood flow in children from 3 to 5 months of age. *AJNR Am J Neuroradiol* 35(3):593-598.
46. Biagi L*, et al.* (2007) Age dependence of cerebral perfusion assessed by magnetic resonance continuous arterial spin labeling. *J Magn Reson Imaging* 25(4):696-702.

47. Tortora D, *et al.* (2017) Prematurity and brain perfusion: Arterial spin labeling MRI. *Neuroimage Clin* 15:401-407.
48. Chiron C, *et al.* (1997) The right brain hemisphere is dominant in human infants. *Brain* 120 (Pt 6):1057-1065.
49. Pelphrey KA, *et al.* (2004) Development of visuospatial short-term memory in the second half of the 1st year. *Developmental psychology* 40(5):836-851.
50. Zhang H, Shen D, & Lin W (2019) Resting-state functional MRI studies on infant brains: A decade of gap-filling efforts. *Neuroimage* 185:664-684.
51. Huttenlocher PR (1990) Morphometric study of human cerebral cortex development. *Neuropsychologia* 28(6):517-527.
52. Marin-Padilla M (1970) Prenatal and early postnatal ontogenesis of the human motor cortex: a golgi study. I. The sequential development of the cortical layers. *Brain Res* 23(2):167-183.
53. Michel AE & Garey LJ (1984) The development of dendritic spines in the human visual cortex. *Hum Neurobiol* 3(4):223-227.
54. Kostovic I, Judas M, Petanjek Z, & Simic G (1995) Ontogenesis of goal-directed behavior: anatomo-functional considerations. *Int J Psychophysiol* 19(2):85-102.
55. Dubois J, *et al.* (2008) Microstructural correlates of infant functional development: example of the visual pathways. *J Neurosci* 28(8):1943-1948.
56. Deoni SC, *et al.* (2011) Mapping infant brain myelination with magnetic resonance imaging. *J Neurosci* 31(2):784-791.
57. Gao W, *et al.* (2015) Functional Network Development During the First Year: Relative Sequence and Socioeconomic Correlations. *Cereb Cortex* 25(9):2919-2928.
58. Wen X, *et al.* (2019) First-year development of modules and hubs in infant brain functional networks. *Neuroimage* 185:222-235.
59. Alcauter S, Lin W, Keith Smith J, Gilmore JH, & Gao W (2015) Consistent anterior-posterior segregation of the insula during the first 2 years of life. *Cereb Cortex* 25(5):1176-1187.
60. Craig AD (2009) How do you feel--now? The anterior insula and human awareness. *Nat Rev Neurosci* 10(1):59-70.
61. Mazzola L, Isnard J, Peyron R, Guenot M, & Mauguiere F (2009) Somatotopic organization of pain responses to direct electrical stimulation of the human insular cortex. *Pain* 146(1-2):99-104.
62. Brothers L, Ring B, & Kling A (1990) Response of neurons in the macaque amygdala to complex social stimuli. *Behavioural brain research* 41(3):199-213.
63. Zilbovicius M, *et al.* (2006) Autism, the superior temporal sulcus and social perception. *Trends Neurosci* 29(7):359-366.
64. Carsin-Vu A, *et al.* (2018) Measurement of pediatric regional cerebral blood flow from 6 months to 15 years of age in a clinical population. *Eur J Radiol* 101:38-44.
65. Greicius MD, *et al.* (2008) Persistent default-mode network connectivity during light sedation. *Hum Brain Mapp* 29(7):839-847.
66. Zilbovicius M, *et al.* (2000) Temporal lobe dysfunction in childhood autism: a PET study. Positron emission tomography. *The American journal of psychiatry* 157(12):1988-1993.
67. Mishra LD (2002) Cerebral blood flow and anaesthesia: a review. *Indian Journal of Anaesthesia* 46(2):87-95.
68. Varela M, Groves AM, Arichi T, & Hajnal JV (2012) Mean cerebral blood flow measurements using phase contrast MRI in the first year of life. *NMR Biomed* 25(9):1063-1072.
69. Licht DJ, *et al.* (2004) Preoperative cerebral blood flow is diminished in neonates with severe congenital heart defects. *J Thorac Cardiovasc Surg* 128(6):841-849.
70. Hardy P, Varma DR, & Chemtob S (1997) Control of cerebral and ocular blood flow autoregulation in neonates. *Pediatr Clin North Am* 44(1):137-152.
71. Tzourio-Mazoyer N, *et al.* (2002) Automated anatomical labeling of activations in SPM using a macroscopic anatomical parcellation of the MNI MRI single-subject brain. *NeuroImage* 15(1):273-289.

512

513

514

515

516

517

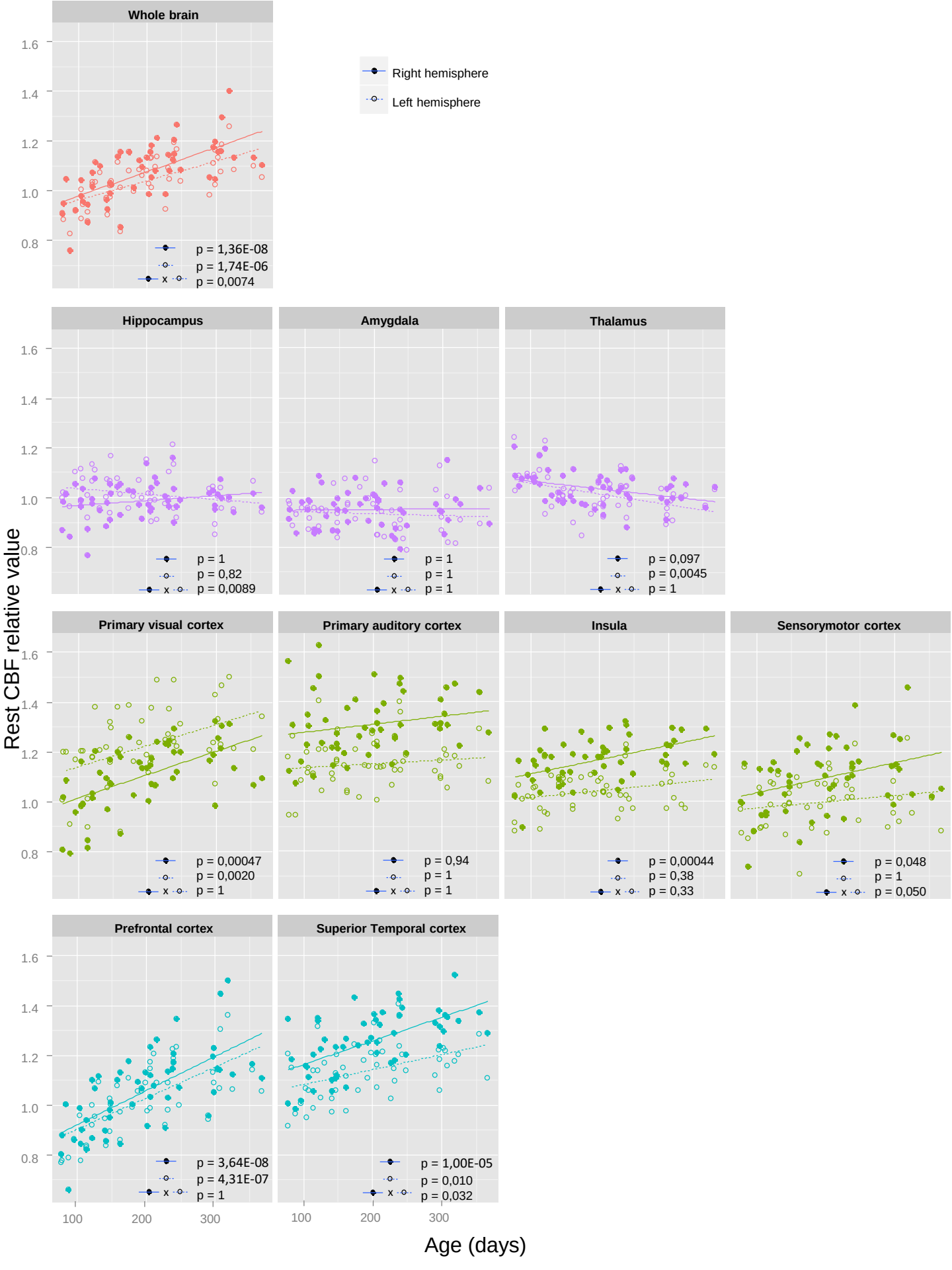
Whole brain
Right hemisphere
Left hemisphere
p = 1,36E-08
p = 1,74E-06
p = 0,0074
Hippocampus
p = 1
p = 0,82
p = 0,0089
Amygdala
p = 1
p = 1
p = 1
Thalamus
p = 0,097
p = 0,0045
p = 1
Primary visual cortex
p = 0,00047
p = 0,0020
p = 1
Primary auditory cortex
p = 0,94
p = 1
p = 1
Insula
p = 0,00044
p = 0,38
p = 0,33
Sensorymotor cortex
p = 0,048
p = 1
p = 0,050
Prefrontal cortex
p = 3,64E-08
p = 4,31E-07
p = 1
Superior Temporal cortex
p = 1,00E-05
p = 0,010
p = 0,032
Rest CBF relative value
Age (days)

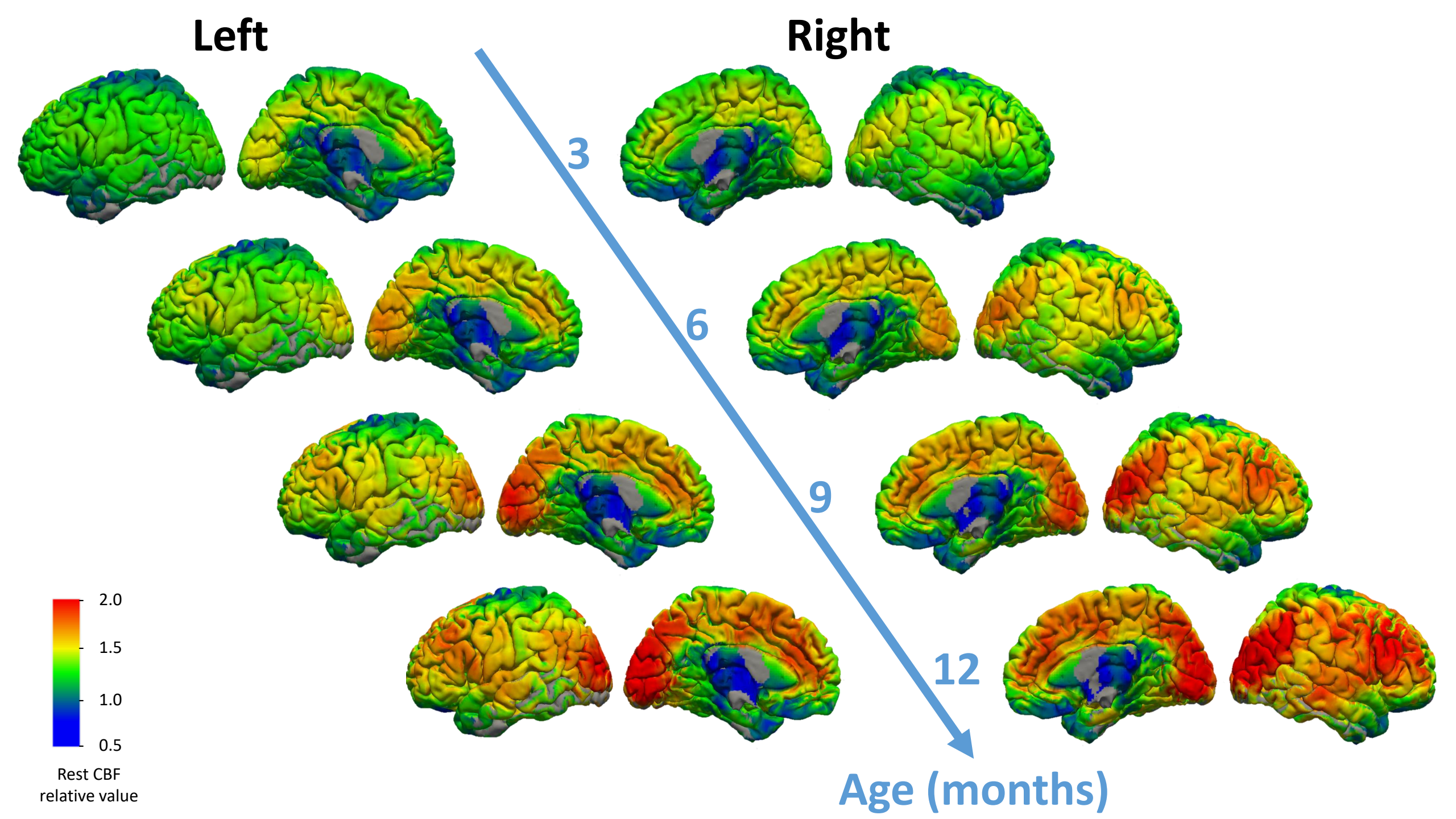
Left
Right
3
6
9
12
Age (months)
2.0
1.5
1.0
0.5
Rest CBF
relative value

Table 1: Age-related changes of the rest CBF values between 3 and 12 months of age.

	Hemisphere	estimate (unit/day)	t(degree of freedom) = t-value	p-value (age)	p-value (age x hemisphere)
Whole brain	Right	0,0010	t(55.71) = 6.64	1,36E-08	0,0074
	Left	0,00078	t(55.71) = 5.34	1,74E-06	
Hippocampus†	Right	0,00019	t(75.14) = 1.52	1	0,0089
	Left	-0,00022	t(75.14) = -1.71	0,82	
Amygdala†	Right	0,000026	t(92.77) = 0.18	1	1
	Left	-0,000076	t(92.77) = -0.54	1	
Thalamus†	Right	-0,00031	t(66.29) = -2.62	0,097	1
	Left	-0,00043	t(66.29) = -3.66	0,0045	
Primary visual cortex†	Right	0,00094	t(59.09) = 4.36	0,00047	1
	Left	0,00085	t(59.09) = 3.94	0,0020	
Primary auditory cortex†	Right	0,00032	t(75.03) = 1.64	0,94	1
	Left	0,00015	t(75.03) = 0.78	1	
Insula†	Right	0,00057	t(82.2) = 4.29	0,00044	0,33
	Left	0,00028	t(82.2) = 2.06	0,38	
Sensorymotor cortex†	Right	0,00061	t(59.33) = 2.89	0,048	0,050
	Left	0,00025	t(59.33) = 1.19	1	
Prefrontal cortex†	Right	0,0014	t(58.9) = 6.9	3,64E-08	1
	Left	0,0012	t(58.9) = 6.26	4,31E-07	
Superior Temporal cortex†	Right	0,00095	t(61.7) = 5.4	1,00E-05	0,032
	Left	0,00060	t(61.7) = 3.41	0,010	

†: p- values Bonferroni corrected for the number of sub-parts of the brain.

rest CBF values are normalized by the rest CBF measured within the basal ganglia and presented in arbitrary unit.